JOURNAL OF SPACECRAFT AND ROCKETS
Vol. 45, No. 3, May–June 2008

Investigation of Actuator Performance for Guiding Supersonic Projectiles

Sidra I. Silton*
U.S. Army Research Laboratory, Aberdeen Proving Ground, Maryland 21005
and
Kevin C. Massey†
Georgia Tech Research Institute, Smyrna, Georgia 30080

DOI: 10.2514/1.34014

A recent study showed that the complex three-dimensional shock/boundary-layer interaction of a pin placed next to a fin produces an asymmetric lift force that can be used for flight control of a projectile. The current study was completed to validate this new technology. A similar projectile was modeled, using high-performance fluid dynamic computations and 6 degree-of-freedom trajectory simulations, to determine the projectile's flight characteristics before being flown in the U.S. Army Research Laboratory's Aerodynamic Experimental Facility. A flight test was designed using this asymmetric lift to produce roll torque. Analysis of the flight data determined that the projectiles with pins developed the expected rolling moments. Computations were completed after the range test on the experimental model for computational validation.

Nomenclature

$C_{l\delta}$ = roll torque coefficient
$C_{\ell p}$ = roll damping coefficient
$C_{m\alpha}$ = pitching moment coefficient derivative
C_{mq} = pitch damping moment coefficient
$C_{N\alpha}$ = normal force coefficient derivative
C_{X0} = zero-yaw drag coefficient
Phi = projectile roll, deg

I. Introduction

THE defense community has recently been interested in guided projectiles that operate in the high supersonic to hypersonic range for various missions. One scenario for missile defense assumes that medium caliber guns (35–75 mm) with high rates of fire could launch multiple supersonic projectiles that could be guided into an incoming missile [1]. For military programs that plan to use high-speed guided munitions, large turning forces may be necessary due to the high closure rates between the projectile and an agile, maneuverable target.

The program discussed herein was conducted as an initial feasibility study for the use of strategically located actuators to provide the necessary turning force to terminally steer a Defense Advanced Research Project Agency (DARPA) command-guided, medium caliber projectile. The actuators were designed to use supersonic adaptive flow control to enhance the divert force generation. Recent studies at Georgia Tech Research Institute (GTRI) [2] have found that the introduction of pins on a projectile in the vicinity of the fins creates shock patterns that impinge on both the fin and body surfaces. The forces created by the shock impingement are capable of providing control forces through asymmetric lift.

Presented as Paper 5195 at the 22nd Applied Aerodynamics Conference and Exhibit, Providence, RI, 16–19 August 2004; received 13 August 2007; accepted for publication 29 October 2007.

*Aerospace Engineer, Aerodynamics Branch, Ballistics and Weapons Concepts Division, Weapons and Materials Research Directorate, Mail Stop AMSRD-ARL-WM-BC. Senior Member AIAA.

†Senior Research Engineer, Aerospace, Transportation, and Advanced Systems Laboratory. Associate Fellow AIAA.

The effort presented here was conducted to validate that placement of pins next to the fins does indeed produce asymmetric lift. Specifically, it was desired to determine if the lift capability of the adaptive flow control technique can be used to create roll torque using two diametrically opposed pins. The creation of sufficient roll torque would produce measurable projectile rotation that can be measured in an aeroballistic facility. The current effort consisted of three parts: 1) high-performance computations to predict projectile behavior due to the presence of the pins for adaptive flow control, 2) an experimental program in an aeroballistic range to determine the asymmetric lift produced by the adaptive flow control technique, and 3) comparison of experimental and computational results for future use.

II. Simulations

Simulations, both computational fluid dynamics (CFD) and 6 degree-of-freedom (6 DOF), were completed before experimental range tests (blind simulations) to determine expected flight characteristics of the projectile. Additional 6 DOF and CFD simulations were completed after the experimental range tests to confirm their accuracy.

A. Computational Fluid Dynamics

CFD simulations were completed using CFD^{++} [3] to obtain force and moment data for the projectiles over a range of supersonic Mach numbers. CFD^{++} solves the Reynolds-averaged Navier–Stokes equations within a finite volume framework. The pointwise k-ε turbulence model [4] was used for the computation of the turbulent flow. Spatial discretization is accomplished using the cell face normal at the cell face centroid, which is obtained by reconstructing the cell centroid values. The point-implicit integration scheme was used to solve the steady-state simulation.

For the simulations completed before the experimental range tests, the full-scale, 50 mm projectile with a tapered leading and trailing fin edge and sharp nose tip was modeled (Fig. 1a). To determine the effect of the control pins on the drag coefficient, simulations were completed on three geometries: a projectile with no control pins (baseline), a projectile with diametrically opposed rectangular control pins, and a projectile with diametrically opposed parallelogram shaped (trapezoidal) control pins (Fig. 1b). These control pins were turned at a 30 deg angle and placed parallel to the fins. The pin shapes and placement correspond to those optimized by GTRI for which limited CFD data had previously been obtained [2].

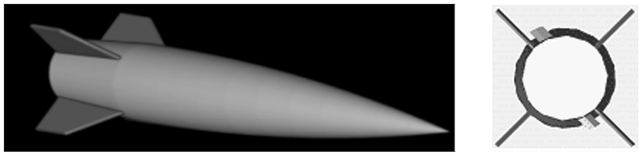

a) b)

Fig. 1 Three-dimensional rendering of models for blind simulations: a) baseline configuration, and b) aft view of projectile with trapezoidal control pins.

The numerical grids for each of these full-scale geometries were supplied by Metacomp Technologies under contract from GTRI. Each grid was unstructured and contained mostly hexahedral cells, with a small number of triangular prisms, and contained approximately 2.9 million cells.

The far-field boundary condition was set to allow the solver to determine the conditions at the far-field boundary (inflow, subsonic outflow, or supersonic outflow) and either explicitly sets the boundary condition to freestream conditions (inflow, subsonic outflow) or extrapolates as necessary (supersonic outflow). Freestream pressure and temperature were set to standard sea level conditions (i.e., 101.325 kPa and 288.15 K, respectively). Density was then calculated from the perfect gas assumption. Velocity was varied between Mach 1.5 and 4.0 and angle of attack was fixed at 0 deg. For the projectile body, fins, and control pins, the boundary condition was set to be a no-slip, adiabatic wall.

B. Six Degree-of-Freedom Trajectory Simulations

Six DOF simulations were completed using the Projectile Design and Analysis System (PRODAS) [5] 6 DOF fixed plane trajectory simulation to determine the number of revolutions the projectile would be expected to complete as it flew down the 100 m aeroballistic range. The physical characteristics of the projectile were specified within PRODAS and a database of aerodynamic coefficients as a function of Mach number was used. For the blind simulations, the database consisted of augmented results from a previously completed flight test using a half-scale 25 mm (baseline) projectile (Fig. 2) launched from a rifled barrel [6]. The augmentation was the change in axial force and rolling moment coefficients due to the presence of the control pins as obtained from CFD. For the simulations completed after the range tests, the database was populated with the aerodynamic coefficients determined during the postprocessing of the range test data.

Initial conditions were specified for the gun and the projectile during setup of the 6 DOF simulation. The gun was set to have an elevation of 0.001 deg and no azimuth. Standard sea level meteorological conditions were used. The gun twist was made extremely large so that the spin at the muzzle was 0 Hz (i.e., smooth bore gun). The initial projectile velocity was varied between Mach 2.0 and 3.0 to match the expected range Mach numbers. The projectile started at the coordinate system origin with no pitch angle, pitch rate, or yaw angle. The initial yaw rate was set to -15.0 rad/s, as this is a typical value for small caliber projectiles. Once the equations of motion were initialized, a fourth-order Runge–Kutta numerical integration scheme was used to integrate the equation of motions in time. The time step was dynamically chosen to account for both pitch frequencies (usually 20 time steps per yaw cycle).

III. Range Tests

Once the initial simulations were completed, flight hardware was designed and built. The baseline projectile was a 25 mm subscale projectile [6] with blunt fin leading and trailing edges, a relatively large fillet between the fins and the body, and a blunt nose tip (Fig. 2). A steel spin pin was inserted in the projectile base to determine the projectile roll position during analysis. The roll torque models (Fig. 3) were created using a control pin of circular cross section, rather than that of the optimized parallelogram shape investigated in the computer simulations, to ease machining requirements on a proof

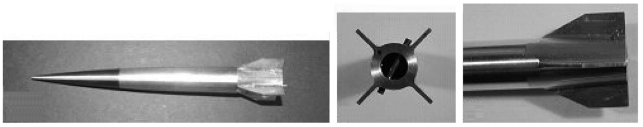

a) b) c)

Fig. 2 Baseline 25 mm projectile as also used in previously completed flight test [6].

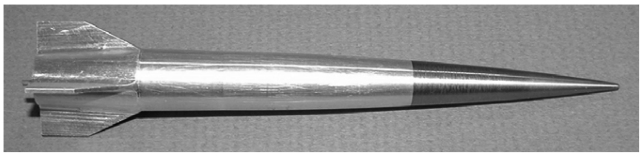

Fig. 3 Photo of short pin model: a) complete projectile, b) base view, and c) closeup of fins.

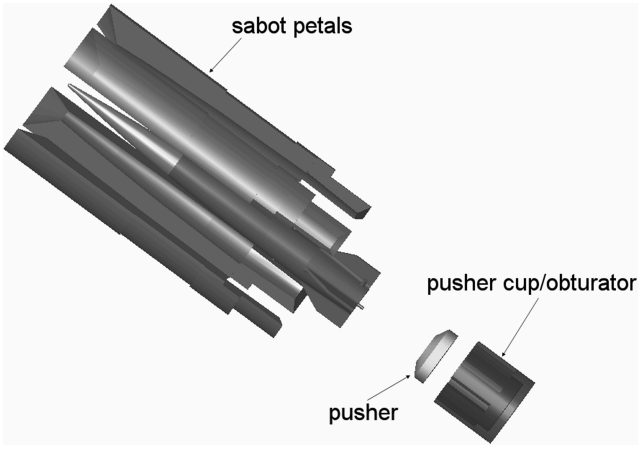

Fig. 4 Exploded three-dimensional rendering of the sabot system with projectile.

of concept experiment. The cylindrical control pins were constructed of 1/16-in.-diam drill rod and machined to 15.0 and 16.7 mm in length to produce the 1.78 mm short control pin model and the 2.54 mm long control pin model, respectively. A hole was drilled through the body to allow for the correct placement of the diametrically opposed control pins (approximately 2.79 mm from the projectile base and a 16 deg rotation from the fin). The chosen rod was fit through the predrilled hole and centered to create two equal length control pins.

To complete the range test, the projectile was encased in a sabot system for launch. The sabot system consisted of four sabot petals, the pusher, and the obturator (Fig. 4). The four sabot petals and the obturator/pusher cup were manufactured from nylon. The pusher was manufactured from 17–4 stainless steel. Each of the four sabot petals had two slots cut out for the fins and control pins. The petals were internally contoured to the projectile shape and fit together to create a cylinder. The pusher cup accommodated the pusher, the sabot petals, and the projectile. The exterior diameter of the pusher cup was flared near the base for an interference fit with the barrel. This allowed for a consistent velocity to be maintained for the charge weight used. The total package weight (projectile and sabot system) was approximately 120 g.

The projectiles were fired from a modified, smooth bore, 25 mm Bushmaster Mann barrel through the range at the U.S. Army Research Laboratory (ARL) Aerodynamic Experimental Facility (AEF). The ARL AEF was designed to evaluate the complete aeroballistics of projectiles as described by Braun [7]. Up to six high-power, orthogonal x rays were used to determine the structural

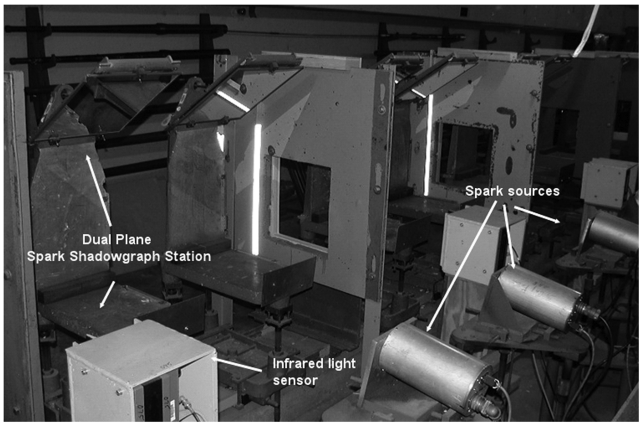

Fig. 5 Photo of dual plane (orthogonal) spark shadowgraph stations with infrared sensor triggers and spark source.

integrity and launch dynamics of the projectile in a manner consistent with other programs [8–10]. The range facility itself consists of 39 orthogonal spark shadowgraph stations (Fig. 5) arranged in five groups over 100 m of trajectory length. Each station provides a vertical and horizontal direct shadow image of the passing projectile at a known time. From these images, the raw data (i.e., the spatial coordinates and angular orientation of the projectile relative to the earth fixed range coordinate system as a function of the spark time) can be obtained.

The raw data were processed with the Aeroballistic Research Facility Data Analysis System (ARFDAS) [11] to determine the aeroballistic coefficients of the configurations. ARFDAS incorporates a standard linear theory analysis and a 6 DOF numerical integration technique. The 6 DOF routine incorporates the maximum likelihood method (MLM) to match the theoretical trajectory to the experimentally measured trajectory. The MLM is an iterative procedure that adjusts the aerodynamic coefficients to maximize a likelihood function. Each projectile fired was initially analyzed separately (single fits), then combined in appropriate groups for simultaneous analysis using the multiple-fit capability. The multiple-fit approach provided a more complete spectrum of angular and translational motion than would be available from any single trajectory.

IV. Results

A. Blind Simulations

Completing the CFD simulations between Mach 1.5 and 4.0 insured data overlap with the previously obtained experimental data [6]. The CFD data were obtained to augment the experimental data set, to account for the increase in drag due to the presence of the control pins and the roll torque created by the control pins. Therefore, although all force and moment data were obtained, the axial force (drag) and roll torque were of primary interest and are presented here.

The drag was determined directly from the axial force coefficient C_{X0}. The presence of the control pins increased the drag over the entire range of Mach number, as expected (Fig. 6). At a given Mach number, the increase in drag due to the presence of the control pins decreased with increasing Mach numbers. The change in C_{X0} with the introduction of the control pins, rather than the absolute magnitude of C_{X0}, is of primary interest, because C_{X0} is known for the baseline shape and must only be augmented.

Because the CFD calculations were completed at 0 deg angle of attack, the roll torque could be directly determined from the axial moment. Figure 7 shows the surface pressure contours for the projectile with rectangular cross section control pins. The shock interactions between the fins and the pins create the areas of high pressure on the fins near the control pins causing the roll torque development. Figure 8 shows that the roll torque coefficient $C_{l\delta}$ decreased by almost 75% over the range of Mach numbers

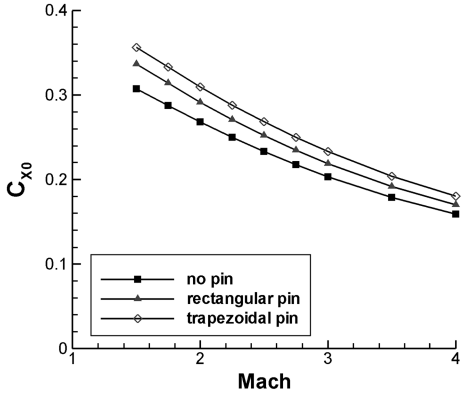

Fig. 6 Computed axial force coefficient vs Mach number.

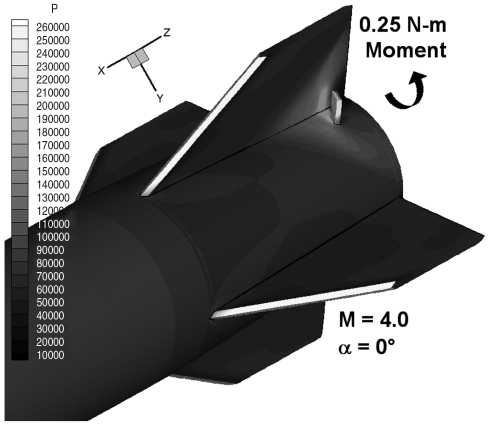

Fig. 7 Surface pressure contours, blind CFD.

investigated. As expected, the trapezoidal control pin created substantially more roll torque over the entire range of Mach numbers.

After completing the CFD for both the rectangular pin and the trapezoidal pin configurations, it was believed that the rectangular pin data would likely be more in line with that of the cylindrical control pins in the planned range test. Hence, the aerodynamic coefficients from the rifled range test [6] were modified by the CFD results of the rectangular control pins.

The 6 DOF simulations were completed at Mach 2.0, 2.5, and 3.0, corresponding to the Mach numbers of the planned range test. The results showed that the projectile could be expected to complete 8–10 turns during the flight downrange depending on Mach number. More revolutions were expected at lower Mach numbers because of the higher roll torque coefficients and due to the fact that the projectile remained in the range for a longer time relative to projectiles traveling at higher Mach numbers due to its lower velocity. Although no dependency on pin length was investigated, an increase in the number of revolutions is expected with an increase in pin length, as an increase in roll torque is expected.

B. Range Test

Up to three Mach numbers were investigated for each configuration, for a total of 15 shots. For the baseline configuration, one projectile was shot for each nominal Mach number of 2.0, 2.5, and 3.0. For the short pin model, three projectiles were shot for each nominal Mach number of 2.0, 2.5, and 3.0. For the long pin model, three projectiles were shot for the nominal Mach number of 3.0.

Gun launch was successful. Consistent velocities were obtained, the sabot petals cleanly separated upon muzzle exit (there was no interference with the projectile motion), and structural integrity of the projectile was maintained. Horizontal and vertical shadowgraph photographs were obtained at each station for each shot. Thus, all aerodynamic coefficients were obtained for each shot.

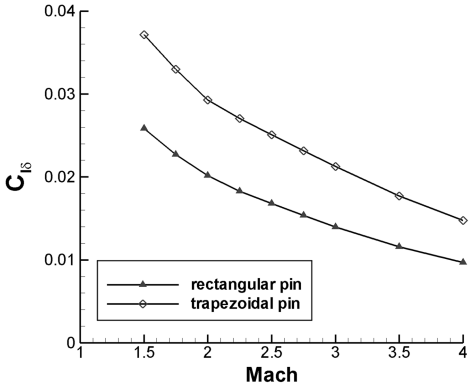

Fig. 8 Computed roll torque coefficient vs Mach number.

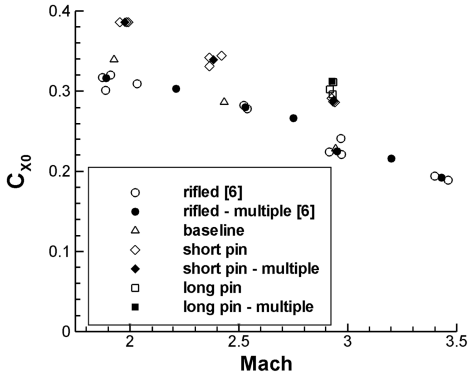

Fig. 9 Experimental zero-yaw axial force coefficient as a function of Mach number.

C_{X0} decreased nearly linearly with Mach number for both the baseline and short pin configuration (Fig. 9). The rifled data shown on the plot are for the baseline projectile geometry and are included to show the consistency between tests. For a given Mach number, C_{X0} increased with the introduction of the control pin, as well as with pin length.

Introduction of the control pin caused the normal force coefficient $C_{N\alpha}$ to increase over that of the original baseline, rifled data. Increasing the length of the control pin may cause an increase in $C_{N\alpha}$. However, there are not enough data available to be conclusive. Additionally, most, but not all, of the shots met the linear theory criterion for good data [12] for $C_{N\alpha}$, as the minimum acceptable yaw levels were exceeded. For shots that did not meet the criterion, $C_{N\alpha}$ was fixed to a reasonable value based on the other data available. This also makes the results inconclusive.

Introduction of the control pins had minimal effect on the pitching moment coefficient $C_{m\alpha}$, though a slight increase in stability can be noticed with the control pins present. Increasing the length of the pin also had practically no effect. The minimal change in $C_{m\alpha}$ and a more pronounced change in $C_{N\alpha}$ for the longer control pin indicate that the center of pressure shifts closer to the center of gravity for the long pin model as compared with the short pin model.

The pitch damping moment coefficient C_{mq} was minimally affected by the introduction of the control pins or the length of the control pins as compared with the results of the rifled test. This was expected, as pin placement was chosen to have minimal effect on pitch damping. C_{mq}, like $C_{N\alpha}$, also has minimum acceptable yaw levels that are necessary to meet linear theory criterion for good data [12]. These minimum acceptable yaw levels were met for most, though not all, shots.

Roll damping and roll torque were the main focus of this range test. Similar to the rifled test, the roll damping coefficient decreased with increasing Mach number. However, the magnitude of the roll damping coefficient $C_{\ell p}$ was found to increase with the introduction of the control pin when compared with a projectile having no control pin. Increasing the length of the control pin, however, reduced the increase. This is likely due to the differences in the shock–shock interactions between the short pin model and the long pin model. The diametrically opposed control pins created roll torque as expected (Fig. 10). The nonzero $C_{l\delta}$ for the baseline case can be accounted for small asymmetries due to the spin pin. For the short pin geometry, $C_{l\delta}$ does not significantly vary with Mach number unlike the other aerodynamic coefficients. At Mach 3, the 50% increase in control pin length nearly doubled the roll torque coefficient. This indicates that there would be a much faster response from the projectile.

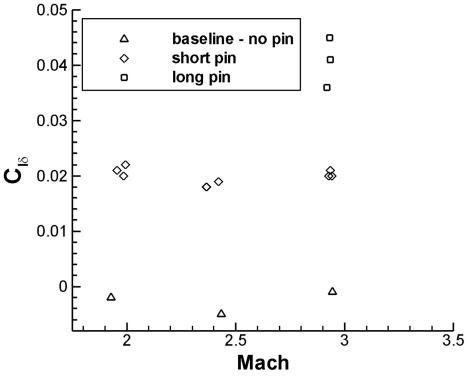

Fig. 10 Experimental roll torque coefficient as a function of Mach number.

The roll rate, which is a balance between the roll torque and the roll damping, increased as the projectile traveled downrange. Although not shown here, the difference in Mach number does not much effect the roll rate. The increase in pin length, however, more than doubles the roll rate by the end of the range.

C. Simulation and Range Test Comparisons

In this subsection, the results of the range test are compared with 1) the blind CFD and 6 DOF simulations, 2) 6 DOF simulations using updated aerodynamics coefficients, and 3) CFD results using matched physical and atmospheric conditions.

1. Blind CFD and 6 DOF

This comparison was completed to determine how well the blind CFD and 6 DOF simulations predicted the range test results despite differences in the geometric model. The differences were not just model size, but also fin leading- and trailing-edge taper (tapered vs blunt), nose bluntness (sharp vs blunt), control pin shape (rectangular vs cylindrical), and relative orientation (parallel vs radial to the fin). Also, the 6 DOF simulations assumed aerodynamic coefficients determined for the baseline projectile shot from a rifled gun tube [6] that were just augmented based on the blind CFD.

A larger C_{X0} for the baseline configuration was observed in the range test than was calculated by the CFD (Fig. 11) and can be attributed to the bluntness of the fins and the nose tip in the experimental model. CFD also underpredicts the increase in C_{X0} due to the presence of the control pin. This is likely due to modeling a rectangular pin parallel to the fin, rather than the experimental cylindrical pin inserted radially to the body. However, augmenting the rifled range test data by the difference between the CFD values for the baseline configuration and the rectangular pin produces a fair estimate of C_{X0} for the short pin projectile.

CFD does well predicting $C_{l\delta}$ despite modeling rectangular, rather than the experimental cylindrical, pins (Fig. 12). The predictions are quite good at Mach 2.0 and 2.5, leading one to believe that the differences in control pin shape are insignificant at these Mach numbers. Perhaps the three-dimensional relieving effects are as significant for the rectangular pins turned at a 30 deg angle and parallel to the fins as for the symmetrically placed circular pins [2]. At Mach 3.0, $C_{l\delta}$ is noticeably underpredicted, indicating that geometric

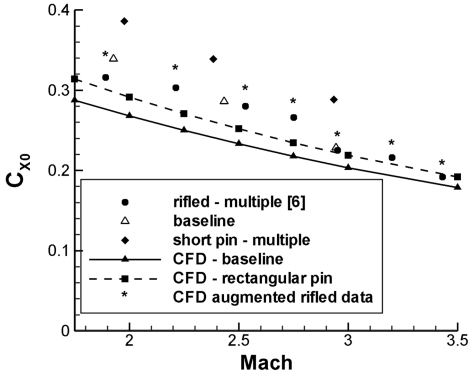

Fig. 11 Axial force coefficient comparison between range test and blind CFD.

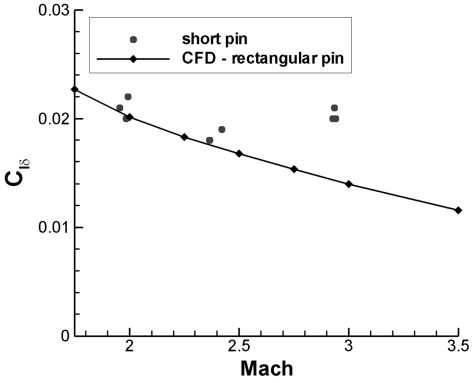

Fig. 12 Roll torque coefficient comparison between range test and blind CFD.

differences and pin placement become important at higher Mach numbers.

As there were differences between the axial force and roll torque coefficients used for the 6 DOF simulation and the values determined by the range test, one expects there to be corresponding differences in the results. This was indeed the case as the number of revolutions achieved at Mach 3.0 was underpredicted at 90 m [8.7 revolutions (revs) vs 7.3 revs], whereas the number of revolutions at the lower Mach numbers was overpredicted at 90 m (6.8 revs vs 7.9 revs at Mach 2.5, and 7.0 revs vs 8.5 revs at Mach 2.0). Regardless, the blind 6 DOF simulations provided a good estimate of what could be expected to occur during the range tests.

2. *Updated 6 DOF*

After completion of the range tests, the 6 DOF simulations were repeated using the aerodynamic coefficients obtained from the range test to populate the database. Very good agreement in both roll rate and, hence, number of revolutions was achieved (Fig. 13), indicating that accurate 6 DOF simulations can indeed be obtained if an accurate aerodynamic coefficient database is available.

3. *Updated CFD*

After completion of the range tests, two new sets of CFD calculations were completed by Metacomp Technologies using the short cylindrical pin model and the long cylindrical pin model. Each computation was completed at 0 deg angle of attack and exactly matched the test conditions of the multiple fit range results for the model, allowing for direct comparison of C_{X0} and $C_{l\delta}$.

CFD accurately determined C_{X0} at all three Mach numbers for both model configurations (Fig. 14). CFD did not do quite as well predicting $C_{l\delta}$ (Fig. 15). CFD predicted a continuous decrease for the short pin model. The range test, however, showed a small decrease in $C_{l\delta}$ between Mach 2.0 and 2.5 with a subsequent increase between

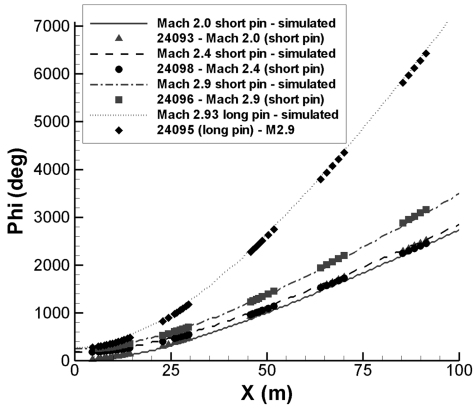

Fig. 13 Comparison of updated 6 DOF and range test results for projectile rotation as a function of distance.

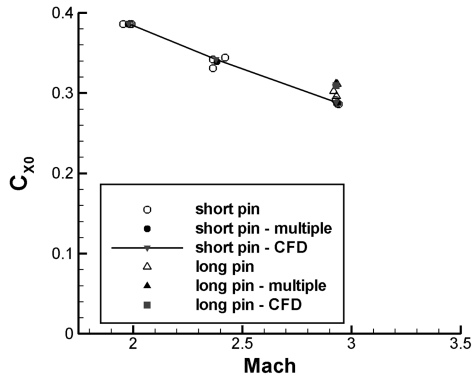

Fig. 14 Comparison of updated CFD to range test zero-yaw axial force coefficient.

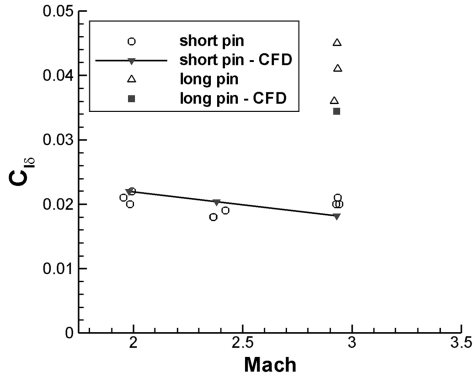

Fig. 15 Comparison of updated CFD to range test roll torque coefficient.

Mach 2.5 and 3.0, resulting in $C_{l\delta}$ being underpredicted at Mach 3.0. It is possible that a nonzero experimental angle of attack or experimental error may be responsible for this discrepancy. For the long pin model, the CFD underpredicts the experimental $C_{l\delta}$, though not always by a significant amount (due to the experimental scatter). The scatter in the range test results suggests an angle-of-attack dependency supporting the hypothesis for the short pin discrepancy.

From CFD visualization, it is possible to see how the pressure disturbances created by the pins on the fins are responsible for the roll torque (Fig. 16 and 17). If one also compares the shock structure predicted by the CFD (Fig. 18) to that seen in the range (Fig. 19), the similarities are easily noticeable. The small differences in the base flow are likely a result of differences in roll orientation, and hence the location of the control pin. Based on the comparison of the updated

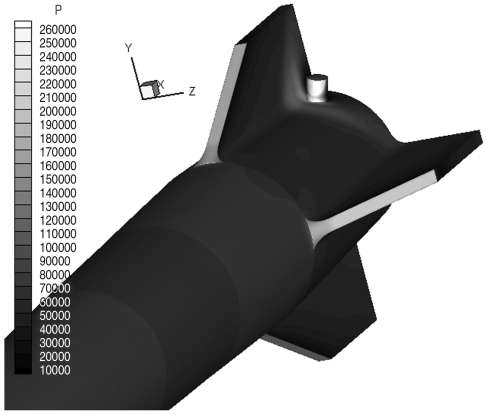

Fig. 16 Surface pressure contours for updated CFD on short pin model at Mach 2.93.

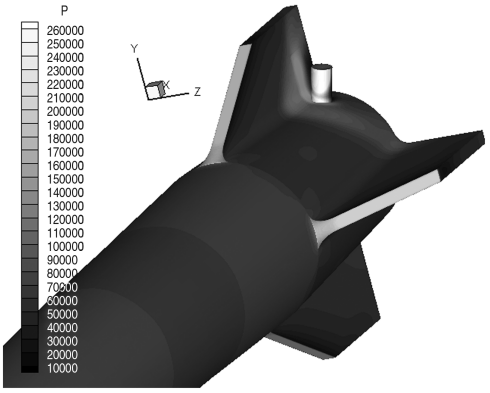

Fig. 17 Surface pressure contours for updated CFD on long pin model at Mach 2.93.

CFD results to the range data, CFD should be able to predict the forces produced by the control pins as the problem is varied (i.e., changes in pin shape, pin location, freestream Mach number).

V. Conclusions

A complete validation program for the use of diametrically opposed pins to produce asymmetric lift was completed. Blind CFD calculations were performed to obtain C_{X0} and $C_{l\delta}$ over a large range of Mach numbers at 0 deg angle of attack for the GTRI optimized control pin configuration. The results of the CFD augmented previously obtained rifled test data. These augmented data were input into a database for use by the 6 DOF trajectory simulations to approximate the results of the range tests.

Flight hardware was designed and built with circular cross section control pins for proof of concept. The flight test was completed and good quality spark shadowgraph photography for data reduction was obtained. Flight-test analysis confirmed that the introduction of diametrically opposed control pins creates roll torque with an increase in drag. As expected, the longer control pin produced a greater amount of roll torque.

Comparison of the blind simulation results to the actual range data was quite good considering differences in geometry (nose, fins, control pins). This shows that the 6 DOF tool in combination with the CFD provides an accurate prediction of the range performance, even when only a preliminary design is available, thereby enabling greater range safety and perhaps a smaller number of actual firings. When the exact geometry and flight conditions were simulated, agreement was quite remarkable. Although the range tests were essential for concept validation, the agreement with CFD means the numerical solutions can be used to visualize the flow phenomena that could not otherwise be obtained, or even investigate the effect of geometry changes on the flow before range testing.

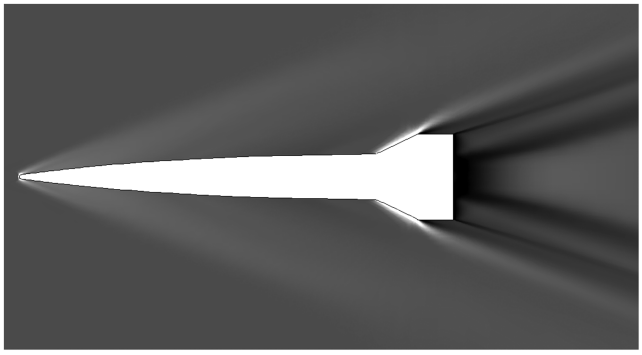

Fig. 18 Pressure coefficient contours through fin symmetry plane for short pin model at Mach 2.93.

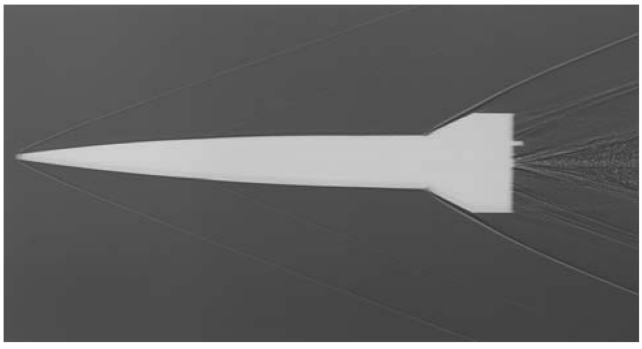

Fig. 19 Shadowgraph at station 27 for short pin model at Mach 2.93.

This integrated approach has shown great promise for the optimization and strategic location of the control pins to achieve the turning force necessary to terminally steer a missile or projectile to its target, thereby increasing the lethality of future combat systems.

Acknowledgments

The authors would like to acknowledge that funding for this project was provided by the Defense Advanced Research Projects Agency Advanced Technology Office. This work was supported in part by a grant of computer time from the Department of Defense High Performance Computing Major Shared Resource Center at the U.S. Army Research Laboratory. The authors would like to thank Metacomp Technologies for providing the grid for the blind computational fluid dynamics and the results for the updated computational fluid dynamics. Finally, the authors would like to thank Peter Plostins for all his help and guidance with the range test and subsequent data reduction.

References

[1] Smith, B. J., Nourse, R. W., Baumann, J. L., and Sanders, G., "Extended Area Protection System (EAPS) Program Overview," *2006 IEEE Aerospace Conference*, Inst.of Electrical and Electronics Engineers Paper 1069, March 2006.

[2] Massey, K. C, McMichael, J., Warnock, T., and Hay, F., "Mechanical Actuators for Guidance of a Supersonic Projectile," *23rd Applied Aerodynamics Conference*, AIAA Paper 05-4970, June 2005.

[3] CFD^{++} User's Manual, Metacomp Technologies, Westlake Village, CA, 2000

[4] Goldberg, U. C., Peromian, O., and Chakravarthy, S., "Wall-Distance-Free k $-$ ε Model with Enhanced Near-Wall Treatment," *Journal of Fluids Engineering*, Vol. 120, No. 3, 1998, pp. 457–462.

[5] Prodas 2000 Technical Manual, South ArrowTech Associates, Burlington, VT, 2001.

[6] Whyte, R., Hathaway, W., and Steinhoff, M., "Aerodynamic Analysis of the Hit-to-Kill (HK) NSWC/ARL Projectile," U.S. Army Research Lab. ARL-CR-501, 2002.

[7] Braun, W. F., "Free Flight Aerodynamics Range," U.S. Army Ballistic Research Lab. BRL-R-1048, 1958.
[8] Plostins, P., Bornstein, J., and Celmins, I. "Effect of Sabot Wheelbase and Positions on the Launch Dynamics of Fin-Stabilized Kinetic Energy Ammunition," U.S. Army Ballistic Research Lab. BRL-TR-3225, 1991.
[9] Plostins, P., Celmins, I., Bornstein, J., and Deibler, J. E., "Effect of Front Borerider Stiffness on the Launch Dynamics of Fin-Stabilized Kinetic Energy Ammunition," U.S. Army Ballistic Research Lab., BRL-TR-3057, 1989.
[10] Bornstein, J., Celmins, I., Plostins, P., and Schmidt, E. M., "Launch Dynamics of Fin-Stabilized Projectiles," *Journal of Spacecraft and Rockets*, Vol. 29, No. 2, 1992, pp. 166–172.
[11] "ARFDAS: Ballistic Range Data Analysis System, User and Technical Manual," ArrowTech Associates, South Burlington, VT, 1997.
[12] McCoy, R. L., *Modern Exterior Ballistic: The Launch and Flight Dynamics of Symmetric Projectiles*, Schiffer Military History, Atglen, PA, 1999, p. 308.

M. Miller
Associate Editor